^{49}Cr: Towards full spectroscopy up to 4 MeV

F. Brandolini,[1] R. V. Ribas,[2] M. Axiotis,[3] M. De Poli,[3] R. Menegazzo,[1] D. R. Napoli,[3] P. Pavan,[1] J. Sanchez-Solano,[4] S. Lenzi,[1] A. Dewald,[5] A. Fitzler,[5] K. Jessen,[5] S. Kasemann,[5] and P. v. Brentano[5]

[1]*Dipartimento di Fisica dell'Università and INFN, Sezione di Padova, Padova, Italy*

[2]*Instituto de Fisica, Universidade de São Paulo, São Paulo, Brazil*

[3]*Laboratori Nazionali di Legnaro-INFN, Legnaro, Italy*

[4]*Departamento de Física Teorica, Universidad Autónoma, Cantoblanco, Madrid, Spain*

[5]*Institut für Kernphysik der Universität zu Köln, Germany*

(Received 22 July 2005; published 17 February 2006)

The nucleus ^{49}Cr has been studied by analyzing γ-γ coincidences in the reaction ^{46}Ti$(\alpha, n)^{49}$Cr at the bombarding energy of 12 MeV. The level scheme has been greatly extended at low excitation energy, and several lifetimes have been determined by means of the Doppler shift attenuation method. Shell model calculations in the full *pf* configuration space reproduce well the negative parity levels. Satisfactory agreement is obtained for positive parity levels by extending the configuration space to include a nucleon-hole in either the $1d_{3/2}$ or $2s_{1/2}$ orbitals. A nearly one-to-one correspondence is found between experimental and theoretical levels up to an excitation energy of 4 MeV. Experimental data and shell model calculations are interpreted in terms of the Nilsson diagram and the particle-rotor model, showing the strongly coupled nature of the bands in this prolate nucleus. Nine values of K^π are proposed for the levels observed in this experiment. As a secondary result, it is shown that the values of the experimental magnetic moments in $1f_{7/2}$ nuclei are well reproduced without quenching the nucleon g factors.

DOI: 10.1103/PhysRevC.73.024313 PACS number(s): 21.10.−k, 21.60.Cs, 21.60.Ev, 27.40.+z

I. INTRODUCTION

In the last few years, the nucleus ^{49}Cr has been studied quite extensively both theoretically and experimentally. It has been shown that shell model (SM) calculations are able to reproduce the ^{49}Cr ground state (gs) band, and that its rotational features at low spin can be described by the particle-rotor model (PRM) as a $K^\pi = 5/2^-$ band based on the $\nu[312]5/2^-$ Nilsson orbital [1]. A rotational behavior was already recognized at low excitation energy in the most recent Nuclear Data Sheets (NDS) compilation [2], which suggested sidebands with $K^\pi = 1/2^-, 3/2^-$ and $3/2^+$, based on $[321]1/2^-$, $[321]3/2^-$ and $[202]3/2^+$ Nilsson orbitals, respectively. More recently, in the framework of research using heavy-ion-induced fusion reactions, evidence of two high-K three-quasiparticle (3-qp) rotational bands with $K^\pi = 13/2^-$ and $K^\pi = 13/2^+$ has been found [3,4]. They have been interpreted with the prolate Nilsson diagram as due to the excitation of a proton to the empty $[312]5/2^-$ orbital from the $[321]3/2^-$ or the $[202]3/2^+$ one, respectively, followed by recoupling of the spins of the three unpaired nucleons to get the maximum value of K.

SM calculations for natural (negative) parity states were made with the code ANTOINE in the full *pf* configuration space [5], and a very good agreement was obtained. Good agreement was achieved for the observed unnatural (positive) parity levels by extending the configuration space to include a hole in the $1d_{3/2}$ orbital. As $B(E2)$ values are an essential mean for evaluating the nuclear deformation, lifetime measurements with the Doppler shift attenuation method (DSAM) were systematically made. A recent review of the SM predictions and their interpretation for most $N \simeq Z$ $1f_{7/2}$ nuclei can be found in Ref. [6].

It has to be noted, however, that in heavy-ion-induced fusion reactions, the population of nonyrast sidebands is weak. As an example, a $K^\pi = 1/2^+$ band, classified as $[200]1/2^+$, was observed in the reaction ^{42}Ca$(\alpha, n)^{45}$Ti about 1 MeV above the $[202]3/2^+$ $K^\pi = 3/2^+$ band [7]. That band was not observed in a subsequent heavy-ion reaction [8] with a much more efficient setup. The knowledge of nonyrast structures is, however, required for a better understanding of nuclear structure. This perspective, often named full spectroscopy, became more important recently, also because some properties of nonyrast states are fingerprints of nuclear symmetries and supersymmetries [9]. Such information was scanty in γ spectroscopy, as levels up to about 2.5 MeV were studied in the reaction ^{46}Ti$(\alpha, n\gamma)^{49}$Cr at a bombarding energy of 8 MeV, more than 25 years ago [10]. We have used the same reaction, but in order to observe nonyrast levels in ^{49}Cr, which are populated with small cross section, a high-efficiency γ-detector array was used. The collected experimental data provide a stringent test for modern SM calculations, as nonyrast levels are more affected by residual interactions and effects of configuration space truncation, because of the increased level density. On the other hand, bands cannot be observed near their smooth terminations, since only states with rather low spin values could be populated. Terminating states in the $1f^n_{7/2}$ and $1d_{3/2} \otimes 1f^{n+1}_{7/2}$ configuration spaces, for natural and unnatural parity bands, respectively, are generally well known from heavy-ion-induced reactions [6].

II. EXPERIMENTAL PROCEDURE

Excited states were populated in the reaction ^{46}Ti$(\alpha, n)^{49}$Cr with the 12 MeV α beam provided by the Cologne

FN-TANDEM accelerator. Five Compton-suppressed Ge detectors and one Compton suppressed CLUSTER detector were used in the COLOGNE-COINCIDENCE-CUBE spectrometer [11]. Four Ge detectors were mounted in the horizontal plane at $\pm 45^\circ$, $\pm 135^\circ$. The fifth Ge detector and the CLUSTER detector were placed along the vertical axis below and above the beam line, respectively. The target consisted of 1 mg/cm^2 ^{46}Ti backed onto 5 mg/cm^2 Au. A total of 200×10^6 γ-γ coincidences were collected in 3 days of beam time.

About 40% of them were due to the reaction being studied. A little less came from the ^{46}Ti(α, p)^{49}V reaction, and nearly 20% came from the inelastic diffusion. Since the target sample contained about 5% ^{48}Ti, minor contributions came from reactions with this isotope. An upper limit was set at about 3.6 MeV in the γ-ray acquisition. This resulted in a limitation for the study of high lying levels, since the production of γ rays with an energy up to 6.6 MeV is allowed by the kinematics. Owing to the detector geometry, precise angular correlation information could not be obtained.

III. DATA ANALYSIS

A. Level scheme

The most useful γ-γ matrices for extending the level scheme have been the two asymmetric ones having all detectors in the first axis and detectors either at $\pm 45^\circ$ (forward or F matrix) or at $\pm 135^\circ$ (backward or B matrix) in the second axis. Many of the observed transitions were either fully Doppler shifted or not Doppler shifted, and the experimental energy resolutions at about 2 MeV were about 7 and 3 keV, respectively. The symmetric γ-γ matrix was used for the analysis of unshifted lines.

A typical analysis of an observed line implied the comparison of spectra obtained with the same gate on backward and forward matrices. The intrinsic energy and the Doppler shift were extracted for all observed transitions by using the most suitable gates for each one. The transitions were placed in the level scheme after comparing spectra for the same direction, but obtained with different gates, and successive cross-checks. One example of the comparison between forward and backward spectra is shown in Fig. 1, where the gate is the 272 keV $7/2^- \rightarrow 5/2^-$ transition. The presence of unshifted, fully shifted, and partially shifted lines is evident. From the analysis of fully shifted lines, one can estimate the average recoil velocity component along the detector axis as 0.45% of c, which corresponds to an average recoil velocity of 0.65% c, in agreement with the kinematics of this reaction.

The adopted level scheme is shown in Fig. 2. All known levels are displayed up to 4 MeV. The few levels that were not observed in the present experiment are not connected by transitions. Above that energy, only levels observed in the present experiment are shown. Levels for which no new information was obtained for spin and parity are displayed with thicker lines. Several high spin levels, elsewhere observed, are not reported [3,4]. In particular, the gs band had been previously observed up to the band termination at $31/2^-$, and the $K^\pi = 13/2^+$ up to $19/2^+$.

Transitions to the ground state from levels directly fed by the reaction cannot be detected in a γ-γ coincidence experiment, so some low-spin states could escape observation if they decay principally to the ground state. This appears to be the case for the $K^\pi = 1/2^-$, $I^\pi = 7/2^-$ level, which is missing in Fig. 2. The transitions of the 2613, 2979, 3251, and 2504 keV levels to the gs were taken from Ref. [2]. Several new levels have been observed above 4 MeV and up to 5.37 MeV, but some others could have escaped observation, if the depopulating transitions had an energy larger than 3.6 MeV. Observed levels and transitions are reported in Table I.

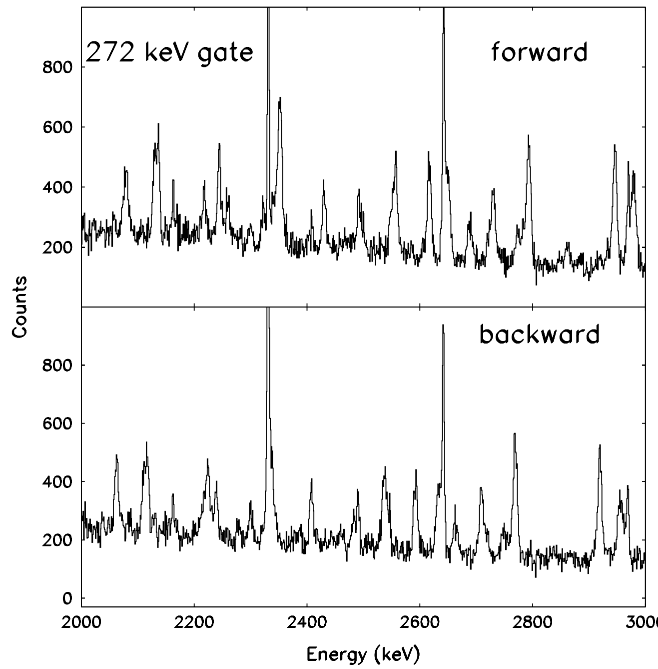

FIG. 1. Spectra obtained by gating on the 272 keV transition in the forward and backward matrices.

Data related to the gs $K^\pi = 5/2^-$ and the $K^\pi = 13/2^+$ bands are not reported since they were already discussed in detail in Refs. [3,4]. In the same table, the branching ratios (BR) are also displayed, in which errors of a systematic contribution of 10% account for angular correlation effects. When possible, they were obtained by gating on a transition directly feeding the level of interest. It is explicitly indicated when gates on transitions below the branches were used, leading to larger uncertainties. Branches that could not be measured are noted, in which case the sum of all branching ratios could not be normalized to 100%. Some variations with respect to NDS are worth noting: (a) The decay from levels $15/2^-$ at 3900 keV and $13/2^+$ at 3893 keV were mixed up in Ref. [12]. (b) The 2160 keV branch of the 2432 keV level is small, in agreement with Ref. [10] and in disagreement with NDS [2]. (c) The previously reported strong branch of 2979 keV from the 3251 keV level [2] was not observed. Most probably that line is produced by the transition of the 2979 keV level to the ground state.

Experimental mixing ratios are not discussed here, since the few reported ones have a large uncertainty [2]. Because of the experimental conditions, only a tentative spin-parity assignment was made for some levels. The proposed spin-parity and K assignments will be justified later.

TABLE I. Experimental data for ^{49}Cr sidebands. $E1$ assignments are based on the observed transition strengths (see text).

E_x (keV)	K value SM orbital	Spin	τ present (ps)	τ previous[a] (ps)	E_γ (keV)	BR previous[a] (%)	BR present (%)	$B(E1)$ estimate ($10^{-4}e^2\,fm^2$)	Parity changing mark
1703	$K^\pi = 1/2^-$	$1/2^-$		>5	1703	100	–		
1742	$2p_{3/2}$	$3/2^-$	>1	1.6(5)	1470[b]	29(3)	–		
					1742	71(3)	–		
2169		$5/2^-$	1.5(5)	>4	427	–	2.1(6)		
					1897*	45(3)	44(5)		
					2169	55(3)	54(5)		
3052		$(9/2)^-$	<0.04		1968	–	56(5)	>6	
					2780	–	44(5)		
					3052	–	–[c]		
3500		$(11/2)^-$	<0.03		2416	–	100	>15	
4105		$(13/2)^-$	<0.03		1604	–	56(5)	>28	
					3021	–	44(5)		
2504	$K^\pi = 7/2^-$	$7/2^-$	<0.03	<0.012	2232[b]	33(5)	–		
	$1f_{7/2}$				2504	67(5)	–		
3202		$(9/2)^-$	<0.04		2118	–	31(6)	>7	
					2930	–	69(6)		
					3202	–	–[c]		
3688		$(11/2)^-$	<0.03		2125	–	31(4)	>9	
					2604	–	69(4)		
4201		$(13/2)^-$	<0.03		1700	–	72(4)	>30	
					3177	–	28(4)		
2613	$K^\pi = 3/2^-$	$3/2^-$		0.06(2)	2341	59(3)	–		
	$1f_{7/2}$				2613	41(3)	–		
3407		$(5/2)^-$				–	–		
3511		$(7/2)^-$			3511	52(10)	–		
					2430	48(10)	–		
3802		$11/2^-$	0.10(3)		1301	–	15(3)		
					2718	–	30(4)		
					3530	–	55(5)		
3528	$K^\pi = 13/2^-$	$13/2^-$	0.48(8)	0.38(7)	337.2	4.0(5)	4.3(9)		
	$1f^3_{7/2}$				1027.6	16(2)	17(3)		
					1965.4[b]	78(3)	79(4)		
					2444.0	1.6(5)	<2		
3900		$15/2^-$	0.40(7)		709*	–	35(5)[d]	12	
					1399*	–	35(5)		
					2337	–	30(5)		
4571		$17/2^-$	0.20(4)		352	–	<5[d]	6	
					1382[b]	–	50(7)		
					2072[b]	–	50(7)		
1982	$K^\pi = 3/2^+$	$3/2^+$	>2	>2.5	240	–	2.4(6)		$E1$
	$1d^{-1}_{3/2}$				279	18(2)	10(2)		$E1$
					1710[b]	11(2)	6(2)		$M2+E3$
					1982	70(2)	81(7)		$E1$
2432		$5/2^+$	1.4(4)	$1.3^{+1.2}_{-0.5}$	450[b]	52(6)	46(6)	25	
					690	–	3.1(6)	0.5	$E1$
					2160	–[e]	1.2(4)	0.01	$E1$
					2432	48(6)	50(6)	0.12	$E1$
2912		$7/2^+$	0.75(15)		480	–	33(5)	34	
					930[b]	–	13(3)		
					2640[b]	–	31(5)	0.19	$E1$
					2912	–	23(4)	0.12	$E1$
3629		$9/2^+$	0.18(4)		717*	–	29(5)	27	
					1197*	–	11(2)		
					2066	–	4.0(6)	0.17	$E1$
					2545	–	25(4)	0.53	$E1$

TABLE I. (*Continued*).

E_x (keV)	K value SM orbital	Spin	τ present (ps)	τ previous[a] (ps)	E_γ (keV)	BR previous[a] (%)	BR present (%)	$B(E1)$ estimate ($10^{-4}e^2$ fm^2)	Parity changing mark
					3357	–	30(5)	0.28	$E1$
4280		$11/2^+$	0.30(6)		651*	–	28(4)†	21	
					1368*	–	42(5)		
					2717	–	17(3)	0.18	$E1$
					3196	–	13(2)	0.08	$E1$
5049		$(13/2^+)$	<0.1		769	–	<10†		
					1420	–	21(3)		
					2548*	–	38(4)		$(E1)$
					3486*	–	41(5)		$(E1)$
2578	$K^\pi = 1/2^+$ $1d_{3/2}^{-1}$	$1/2^+$	>1		596	–	12(3)		
					836*	62(5)	57(7)	<6	$E1$
					875*	38(5)	30(5)	<3	$E1$
2979		$(3/2^+)$	>1		401*	–	59(8)		
					547*	–	100		
					810	–	40(5)	<3.9	$(E1)$
					997*	–	27(4)	<1.4	$(E1)$
					1237	–	25(4)	<0.7	$(E1)$
					2979	–	–[c]		$(E1)$
3251		$5/2^+$	0.20(5)		819*	–	44(6)	17	
					1269*	77(5)	44(6)	6	
					2979	–[e]	<5	<0.04	$E1$
					3251	23(5)	12(3)	0.07	$E1$
3844		$(7/2^+)$	0.30(6)		1412*	–	100		
					3572	–	–[c]		$(E1)$
					3844	–	–[c]		$(E1)$
4297		$(9/2)^+$	0.05(2)		1385*	–	100		
					4025	–	–[c]		$(E1)$
4944		$(11/2)^+$	0.07(2)		1315*	–	100		
					3860	–	–[c]		$E1$
3893	$K^\pi = 13/2^+$ $1d_{3/2}^{-1}1f_{7/2}^2$	$13/2^+$	>10		364.4	22(2)	17(3)	<2	$E1$
					701.9	18(2)	18(3)	<0.3	$E1$
					2330.0	60(2)	65(4)	<0.03	$E1$
4052	$K^\pi = (7/2^+)$ $1d_{3/2}^{-1}1f_{7/2}^2$	$(9/2^+)$	0.26(4)		1140	–	10(2)	2	
					2489*	–	27(4)	0.5	$(E1)$
					2968*	–	63(6)	0.7	$(E1)$
4460		$(11/2^+)$	0.23(4)		3376	–	100	0.8	$(E1)$
4717		$(13/2^+)$	0.70(10)		2216*	–	56(8)	0.5	$(E1)$
					3154*	–	44(8)	0.1	$(E1)$
	Others								
4749			<0.05		2248	–	41(8)		
					3186*	–	59(8)		
4810			<0.05		1619*	–	44(8)		
					2309	–	56(8)		

[a]From Ref. [2], except for levels at 3528 and 3893 keV [3].
[b]For these transitions, a DSAM analysis was performed.
[c]This line could not be observed.
[d]Branchings of this level were evaluated gating on lower transitions.
[e]Contaminated lines: Branching ratios (BR) are reported to be large in the NDS, while they are very small in the present work.

B. Lifetimes and electromagnetic reduced rates

For DSAM lifetime determinations, the program LINESHAPE has been used [13] and the Northcliffe-Schilling stopping power [14], corrected for atomic shell effects [15], was adopted. Spectra gated from transitions below the ones examined were used (i.e., the standard procedure) since the experimental conditions did not allow the use of the narrow gate on transitions below (NGTB) procedure, which does not depend on the sidefeeding time of the examined level [16]. In this work, the sidefeeding was assumed to occur

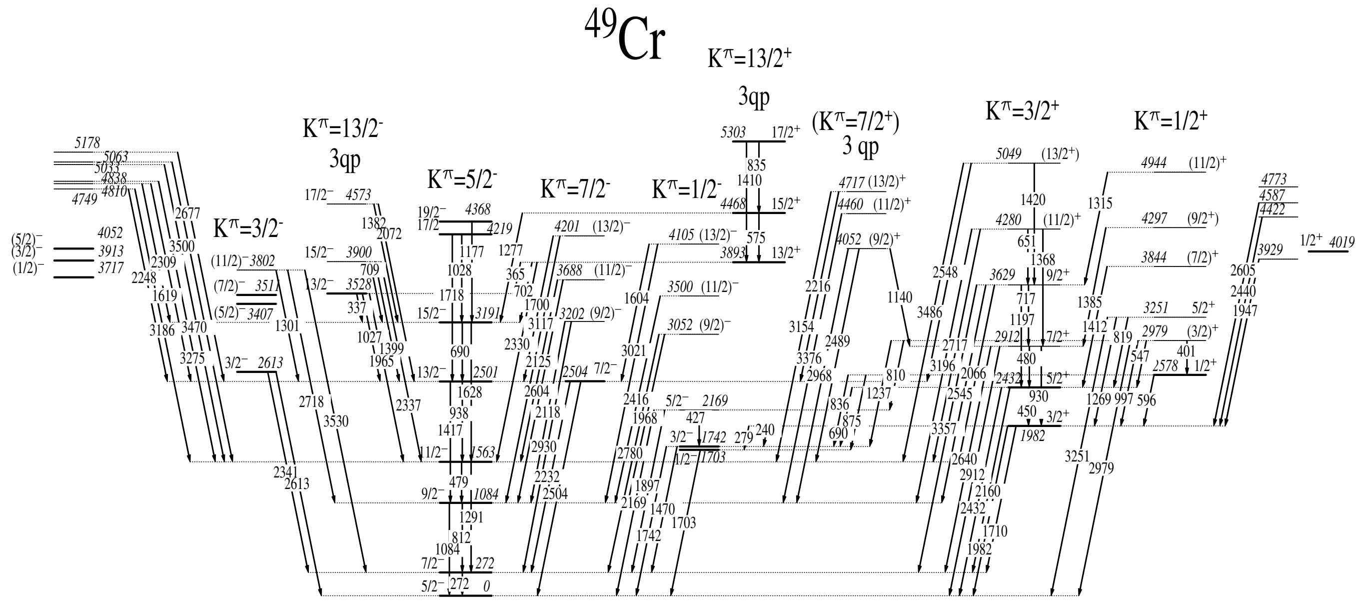

FIG. 2. Experimental ^{49}Cr level scheme. All experimental levels are reported up to about 4 MeV, while only levels observed in this work are reported at higher energies. Levels previously known are represented with thicker lines. Only observed transitions are reported apart for the ones of 2613, 2979, 3251, and 2504 keV, taken from Ref. [2]. The suggested assignments of the levels $9/2^-$, $11/2^-$, and $13/2^-$ to the bands $K^\pi = 1/2^-$ and $7/2^-$ may be interchanged.

instantaneously at the reaction time. This is corroborated by the observed large number of full shifted lines. Examples of DSAM analysis are shown in Figs. 3 and 4.

Obtained lifetimes for bands not yet studied [3,17] are reported in Table I, while the deduced $B(E2)$ and $B(M1)$ values are shown in Table II. In order to check the reliability of the presently obtained values, the lifetime of the $13/2^-$ yrast level was reevaluated to be 0.17(2) ps, in agreement with the previously obtained value of 0.15(2) ps [4].

In order to determine the level parities, the upper limit (UL) of 3×10^{-4} W.u., extracted from data for several nuclei in this region in Refs. [3,4,17–21], was adopted for $E1$ transitions, for which such a criterion was found to be very successful. The $B(E1)$ values of most relevant transitions are reported in the last but one column of Table I in units of 10^{-4} e^2 fm^2, which is approximately 1 W.u. Therefore, the $E1$ assignment is excluded for transitions for which $B(E1)$ values exceed 3×10^{-4} e^2 fm^2.

If the $B(E1)$ value is lower, the $M1 + E2$ character cannot be excluded, but in some cases it is unfavored. The proposed $E1$ assignments are reported in the last column of Table I.

IV. DISCUSSION

A. Particle-rotor model

In a previous work, a deformation parameter $\beta \simeq 0.26$ was deduced for the low members of the ^{49}Cr gs band [3]. The most used formulas for describing the properties of deformed nuclei are those related to the rigid axial rotor.

As for the electromagnetic (em) moments, they are well known in the case of a definite value of the spin projection K

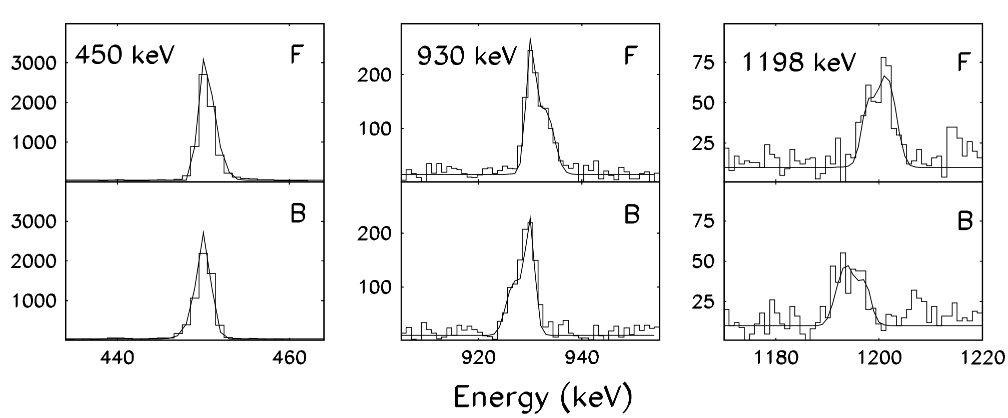

FIG. 3. Examples of DSAM lineshape analysis along the $K^\pi = 3/2^+$ band.

TABLE II. Experimental and SM reduced rates. Parity is nonchanging. When the sum of branching ratios (BR) is less than 1, the theoretical lifetime has to be compared with the experimental one divided by the BR sum.

γ line[a]	E_γ exp. (keV)	E_γ SM (keV)	γ-BR adopted (%)	γ-BR SM (%)	τ adopted (ps)	τ SM (ps)	$B(E2)$ rotor (e^2 fm^4)	$B(E2)$ exp. (e^2 fm^4)	$B(E2)$ SM e^2 fm^4	$B(M1)$ exp. μ_N^2	$B(M1)$ SM μ_N^2
$K = 1/2^-$											
$1/2 \to 5/2$	1703	1464	100	100	>5	27		>0.4	2.1		
$3/2 \to 5/2$	1742	1472	71(3)	75	1.6(5)	12			3.25		0
$3/2 \to 7/2$	1470	1192	28(3)	25					2.28		–
$3/2 \to 1/2$	(39)	8	<0.1	0			234		241		0.165
$5/2_2 \to 5/2$	2169	1873	54(3)	55	1.5(5)	2.3		6.1	4.12	0.002	0
$5/2_2 \to 7/2$	1897	1594	44(3)	45				9.7	2.5	0.002	0.001
$5/2_2 \to 1/2$	(465)	409	<0.1				233		252		–
$5/2_2 \to 3/2$	427	401	2.1(5)				65		69	0.009	0.001
$7/2_2 \to 5/2$	(2504)[b]	2299			<0.012	0.21			0.3		0.011
$7/2_2 \to 7/2$		2020							1.5		0.012
$7/2_2 \to 9/2$		1114							4.9		0.013
$7/2_2 \to 3/2$		826					240		306		–
$7/2_2 \to 5/2_2$		425					25		32.9		0.160
$9/2_2 \to 5/2$	(3052)	2753	0	4	<0.04	0.37			0.3		–
$9/2_2 \to 7/2$	2780	2474	44(6)	20					3.6		0
$9/2_2 \to 9/2$	1968	1569	56(6)	68					51		0
$9/2_2 \to 5/2_2$	(883)	880	0	8			300		350.2		–
$9/2_2 \to 7/2_2$	548	455		0			46		17.9		0
$9/2_2 \to 7/2_3$	548	228		0					0.2		0
$K = 7/2^-$											
$7/2_3 \to 5/2$	2504	2525	67(9)	79	<0.012	0.003			52.1		0.981
$7/2_3 \to 7/2$	2232	2246	33(9)	21					17.9		0.372
$7/2_3 \to 9/2$	(1420)	1340	<5	0					0.5		0.004
$7/2_3 \to 5/2_2$	(335)	652	<5	0					0.14		0.001
$9/2_3 \to 5/2$	(3202)	3147	0	0	<0.03				3.4		–
$9/2_3 \to 7/2$	2930	2868	69(6)	73					0.5		0.529
$9/2_3 \to 9/2$	2118	1963	31(6)	26					5.1		0.500
$9/2_3 \to 5/2_2$	1033	1275	0	0			253		1.9		–
$9/2_3 \to 7/2_2$	(698)	850	0	0					1.4		0.008
$9/2_3 \to 7/2_3$	(698)	622	0	0			279		185.5		0.534
$K = 3/2^-$											
$3/2_2 \to 5/2$	2613	2435	59(3)	68	0.06(2)	0.18			2.7		0.012
$3/2_2 \to 7/2$	2341	2156	41(3)	32					20.3		–
$5/2_3 \to 3/2_2$	(894)	842	–				340		5.2		0.142
$7/2_4 \to 5/2$	(3511)	3380	52(10)	45		0.008			4.6		0.071
$7/2_4 \to 7/2$	(3239)	3100	0	15					16.8		0.018
$7/2_4 \to 9/2$	(2430)	2195	48(10)	40					20.0		0.186
$7/2_4 \to 3/2_2$	(898)	0	0				179		67.8		–
$7/2_4 \to 5/2_3$	(104)	0	0				269		38.1		0.096
$K = 13/2^-$											
$13/2_2 \to 11/2$	1965	1815	78(3)	64	0.42(6)				1.1	0.010	0.004
$13/2_2 \to 13/2$	1027	846	16(2)	32					0.8	0.025	0.014
$13/2_2 \to 15/2$	337	225	4.0(5)	4					14.3	0.12	0.044
$15/2_2 \to 11/2$	2337	2313	35(5)	25	0.40(7)			11.6	11.2		–
$15/2_2 \to 13/2$	1399	1345	35(5)	50					20.5	0.016	0.040
$15/2_2 \to 15/2$	709	753	30(5)	25					40.3	0.118	0.146
$15/2_2 \to 13/2_2$	(372)	499	<5						137.6		0.012
$17/2_2 \to 13/2$	2072	2098	50(7)	40	0.20(4)	0.34		50	24.7		–
$17/2_2 \to 15/2$	1382	1506	50(7)	60					2.0	0.054	0.038
$17/2_2 \to 13/2_2$	(1045)	1251	0	0					27.4		–
$17/2_2 \to 15/2_2$	(673)	752	0	0					152		0
$K = 3/2^+$											
$5/2 \to 3/2$	450	547	46(6)		1.4(4)	3.3	340		284.4	0.178	0.070

TABLE II. (*Continued*).

γ line[a]	E_γ exp. (keV)	E_γ SM (keV)	γ-BR adopted (%)	γ-BR SM (%)	τ adopted (ps)	τ SM (ps)	$B(E2)$ rotor (e^2 fm^4)	$B(E2)$ exp. (e^2 fm^4)	$B(E2)$ SM e^2 fm^4	$B(M1)$ exp. μ_N^2	$B(M1)$ SM μ_N^2
$7/2 \to 3/2$	930	905	13(3)	38	0.75(15)	2.6	179	203	175.7		–
$7/2 \to 5/2$	480	358	33(5)	62			269		247.6	0.220	0.125
$9/2 \to 5/2$	1197	1098	11(2)	43	0.18(4)	0.68	269	202	210.2		–
$9/2 \to 7/2$	717	740	29(5)	57			176		88.0	0.148	0.127
$11/2 \to 7/2$	1369	1148	42(5)	79	0.30(6)	0.53	319	330	256.4		–
$11/2 \to 9/2$	651	408	28(4)				123		107.0	0.159	0.081
$K = 1/2^+$											
$1/2 \to 3/2$	596	544	12(3)		>1	55			124.8		0.0016
$3/2_2 \to 3/2$	997	1068	15(2)[c]	73	>1	0.76			17.6		0.055
$3/2_2 \to 5/2$	547	521	54(6)[c]	11					54.6		0.052
$3/2_2 \to 1/2$	401	524	31(5)[c]	16			251		164.8		0.179
$5/2_2 \to 3/2$	1269	1314	44(6)	85	0.30(6)	0.12			21.9	0.041	0.101
$5/2_2 \to 5/2$	819	840	44(6)	15					0.8	0.152	0.132
$5/2_2 \to 1/2$	(673)	770	0	0			251		194.6		–
$5/2_2 \to 3/2_2$	(272)	246	0	0			72		88.9		0.393

[a]Subscripts to spin values refer to the calculated levels in Fig. 6.
[b]Data for the observed $7/2^-$ level, assigned to $K = 7/2^-$, are inserted only into the $K = 1/2^-$ band, for a comparison.
[c]The sum of branchings may be less than 1 if there is an $E1$ branch to the gs.

along the intrinsic symmetry axis, according to the rotor model [22]. The intrinsic electric quadrupole moment $Q_\circ$ is related to the spectroscopic one Q_s by the relation

$$Q_s = Q_\circ \frac{3K^2 - I(I+1)}{(I+1)(2I+3)}. \quad (1)$$

The intrinsic quadrupole moment can also be derived from the $B(E2)$ values, where it is usually denoted as Q_t:

$$B(E2) = \frac{5}{16\pi} Q_t^2 \langle I_i K 20 | I_f K\rangle^2. \quad (2)$$

Concerning the magnetic properties, the g factor of a level with $K \neq 1/2$ is related to the collective g factor g_R and to the intrinsic value g_K by the formula

$$g = g_R + (g_K - g_R)\frac{K^2}{I(I+1)}. \quad (3)$$

For $M1$ transitions, one has similarly

$$B(M1) = \frac{3}{4\pi} \langle I_i K 10 | I_f K\rangle^2 (g_K - g_R)^2 K^2 \mu_N^2. \quad (4)$$

The $B(E2)$ values within a band are sensitive to the K value via the Clebsch-Gordan coefficient. This is also the case of Q_s, which, however, is rarely known experimentally. The value of the deformation parameter is assumed to be given by the formula $Q_t = 1.09 Z A^{2/3} \beta(1 + 0.36\beta)\,\mathrm{fm}^2$, which accounts for nuclear volume conservation in the case of deformation [23]. Equations (3) and (4) show that the magnetic properties are sensitive to the nature of the involved quasiparticles.

These formulas provide mostly a qualitative interpretation tool, since the assumption of a pure value of K is not valid in general. In fact, even under the extreme hypothesis that the unpaired neutron does not interact singularly with the other

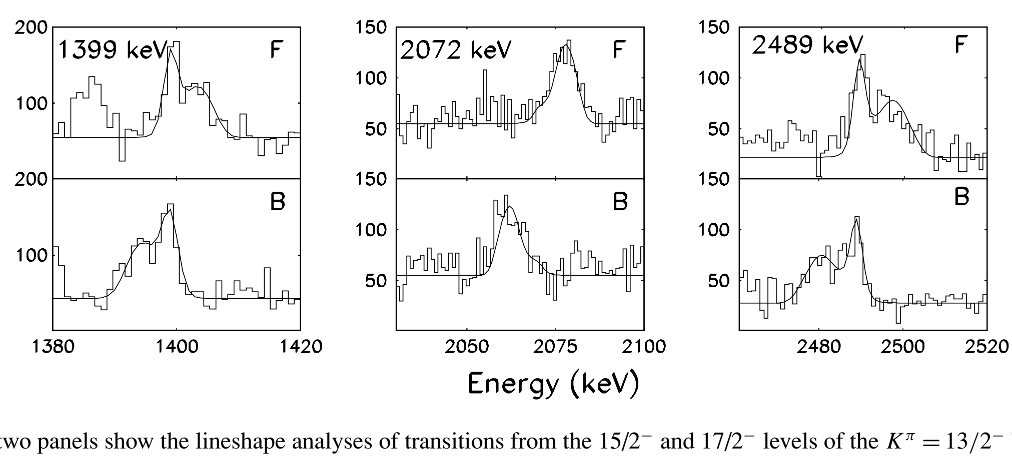

FIG. 4. First two panels show the lineshape analyses of transitions from the $15/2^-$ and $17/2^-$ levels of the $K^\pi = 13/2^-$ band, respectively. The last panel refers to a transition from the $(9/2^+)$ level attributed to the $K^\pi = (7/2^+)$ band.

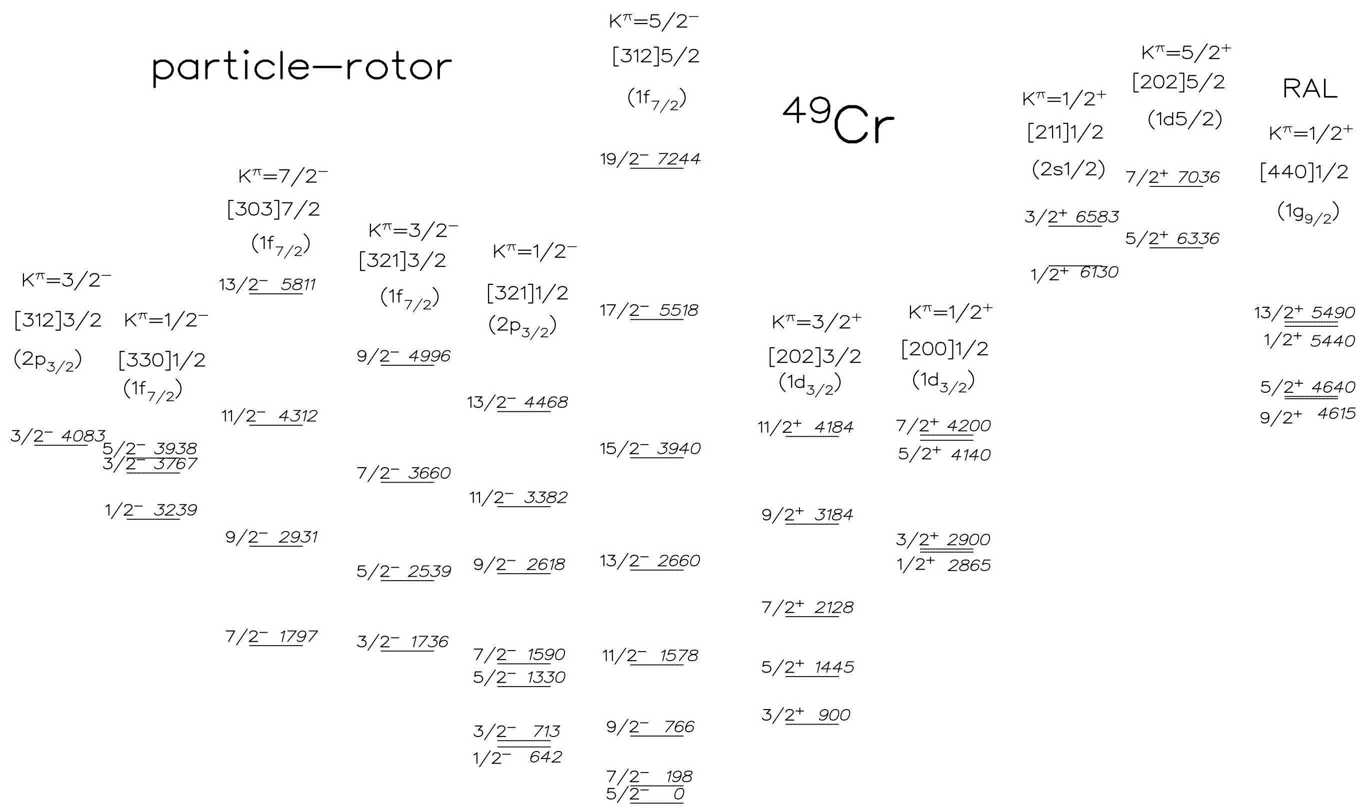

FIG. 5. Particle-rotor predictions in ^{49}Cr assuming axial symmetry and $\beta = 0.26$.

nucleons, one has to account for the coupling of the spin of the neutron with the rotational moment in order to conserve the total angular moment I. This is made by the particle-axial rotor model (PRM), according to which K is not a good quantum number because of the Coriolis force.

Figure 5 shows the level scheme predicted by the PRM at low excitation. The bands are identified with the dominant Nilsson configuration. For PRM calculations, the code of Ref. [24] was used, which can also describe the coupling of a particle with a triaxial rotor. The standard set of parameters for an axial symmetry were here adopted together with the 2^+ level energy of the ^{48}Cr core, without any further adjustment of parameters. Apart from the fact that the PRM model cannot predict the observed 3-qp bands, there is correspondence with most observed low lying levels up to about 4 MeV, which are reported in Fig. 2. The agreement can only be qualitative, owing to the shortcoming of the model, in particular the disregard for any residual interaction. Nevertheless, a comparison serves as a means to propose for the observed levels the K^π values reported in Fig. 2.

The assumption of collective triaxiality cannot reproduce the size of the observed gs-band signature splitting. Cranked shell model (CSM) calculations predict some signature splitting for a collective triaxiality, i.e., with a negative sign for the deformation parameter γ in the Lund convention, but its size is also insufficient.

A further limitation of the particle-rotor model is that it cannot explain the backbending of the gs band at $I = 19/2$, which was interpreted as a termination of seniority 3 configurations and thus as an effect of the competition of the seniority scheme with rotational collectivity [25,26].

Other negative parity bands built with *pf* configurations are expected above 4 MeV such as those based on the [301]1/2$^-$, [301]3/2$^-$, and [303]5/2$^-$ orbitals. Because of the configuration mixing, interband transitions are generally predicted to prevail over intraband ones, owing to the larger transition energies, thus qualitatively explaining why few intraband transitions have been observed.

The Q_s and g values calculated with PRM are compared with the rotor predictions of Eqs. (1) and (3) in Table III. The latter values were obtained with the PRM, multiplying the Coriolis coupling term by a null factor. The staggering of g factor values predicted for $K^\pi = 1/2^-$ is caused by the contribution of the decoupling factor to Eq. (3). The predicted level scheme keeps, nevertheless, the strongly coupled appearance. In Eqs. (3) and (4), $g_R = 0.5$ is taken and the suggested 0.6 quenching factor is assumed for the nucleon g factor [24]. A particularly strong mixing occurs between levels close in energy, as for the head of the $K^\pi = 7/2^-$ band, near to the 7/2$^-$ level with $K = 1/2$, in which case the PRM g-factor value is slightly positive while the rotor one is negative.

Concerning positive parity levels, "extruder" bands $K^\pi = 3/2^+$ and $1/2^+$ are expected at low excitation energy, being based on the [202]3/2$^+$ and [200]1/2$^+$ orbitals, respectively. Such bands have been observed at low energy in the nucleus ^{45}Ti, where they have been satisfactorily described by PRM [7]. The 3/2$^+$ level at 1982 keV is strongly excited by $\ell_n = 2$

TABLE III. Theoretical Q_s and g-factor values in single-particle bands. $g_s^{\text{eff}} = 0.6 g_s$ was assumed in PRM and rotor evaluations.

K	Spin	Q_s			g factor		
		PRM	Rotor	SM	PRM	Rotor	SM
$5/2^-$	5/2	36.1	35	36.3	−0.27	−0.14	−0.20
	7/2	11.6	8.2	9.6	0.14	−0.07	−0.01
	9/2	−6.8	−8.7	−8.4	0.02	0.27	0.23
$1/2^-$	1/2	0	0	0	1.11	1.13	0.848
	3/2	−21.5	−20	−22.3	−0.24	0.02	−0.23
	5/2	−30.8	−29	−32.8	0.55	0.73	0.47
	7/2	−17.4	−33	−36.6	0.04	0.28	0.20
	9/2	−33.6	−36	−40.6	0.42	0.64	0.43
$7/2^-$	7/2	23.1	46	31.7	0.04	−0.15	0.10
	9/2	3.7	18	8.3	0.23	0.08	0.28
	11/2	−9.7	1	−1.0	0.28	0.21	0.41
$3/2^-$	3/2	22.0	19	22.5	−0.08	−0.17	−0.42
	5/2	−4.6	−8.1	−14.6	0.36	0.23	0.83
	7/2	−16.8	−22.5	−9.3	0.48	0.43	0.34
$3/2^+$	3/2	21.5	22.5	21.4	0.552	0.57	1.06
	5/2	−8.7	8.0	12.2	0.501	0.52	0.74
	7/2	−24.0	−22.5	−14.3	0.497	0.51	0.749
$1/2^+$	1/2	0	0	0	−0.554	−0.56	−1.06
	3/2	−21.5	−22.5	−20.2	0.682	0.67	0.66
	5/2	−31.4	−32.1	−20.0	0.312	0.29	0.54

pickup in ^{50}Cr. This agrees with the PRM prediction that the $[202]3/2^+$ orbital has a nearly pure $1d_{3/2}$ hole configuration. Similarly, the yrast $1/2^+$ level at 2578 keV is clearly the bandhead of the $K^\pi = 1/2^+$ band based on the $[200]1/2^+$ hole configuration as it is strongly excited by the $\ell_n = 0$ pickup reaction on ^{50}Cr [2]; but in this case, the orbitals $[200]1/2^+$ and $[211]1/2^+$ share the $\ell_n = 0$ component to a comparable amount.

The first positive parity SM orbital above the Fermi level is $1g_{9/2}$. In the deformed nucleus ^{49}Cr, the lowest intruder level of positive parity is expected to be the $9/2^+$ one belonging to the decoupled band based on the $\nu[440]1/2^+$ orbital. Since this level can be described to a large extent with the configuration $^{48}\text{Cr} \otimes \nu g_{9/2}$ it should be strongly excited in a neutron stripping reaction, which is not feasible since ^{48}Cr is unstable. In ^{51}Cr, a level is observed at an excitation energy of 4.16 MeV in the $^{50}\text{Cr}(d, p)$ reaction with a large $\ell_n = 4$ spectroscopic factor of $S_n = 3.2$, and it is thus described with a dominant $^{50}\text{Cr} \otimes \nu g_{9/2}$ configuration. However, the expected band is not yet observed with γ spectroscopy. Since the deformation of ^{50}Cr is comparable with that of ^{48}Cr [17], the decoupled band in ^{49}Cr should start above 5 MeV, because the sloping up $\nu[312]5/2^-$ orbital is empty in ^{48}Cr. We estimate, therefore, that it is out of the sensitivity range of the present experiment.

1. Questions related to isospin

It is worth noting that the hole excitations giving rise to the bands $K^\pi = 3/2^+$ and $1/2^+$ are not of pure neutron character, as assumed in the PRM, since isospin conservation implies a proton-hole contribution of one-third for the yrast states $3/2^+$ and $1/2^+$.

Since the lowest $T = 3/2$ state, the isobaric analog state (IAS) of the $7/2^-$ ^{49}V gs, lies at 4764 keV, the following comparison of ^{49}Cr levels with SM theoretical levels will be limited to states of the lowest isospin $T = 1/2$.

A few comments are added on higher IAS's. The $T = 3/2$ state IAS of the yrast $3/2^+$ in ^{49}V lies at 5573 keV in ^{49}Cr [27]. In this reference, the sum of the $\ell_n = 2$ pickup strengths of the $3/2^+$ IAS's in ^{45}Ti and ^{49}Cr was probably somewhat overestimated because some contribution of the $[202]5/2^+$ orbital, expected at similar energies, was likely included. A large experimental $\ell_n = 0$ pickup strength is concentrated on a level at 6470 keV, which was interpreted as the $T = 3/2$ IAS of the yrast $1/2^+$ in ^{49}V. The ^{49}Cr $1/2^+$ level with configuration $[211]1/2^+$ is predicted more than 3 MeV above the one based on the $[200]1/2^+$ orbital, but it is likely fragmented owing to the high level density, while IAS's are more robust against mixing. It may be that some $\ell_n = 0$ strength due to the $[211]1/2^+$ orbital was attributed to IAS fragmentation of the $T = 3/2$, $I^\pi = 1/2^+$ state, leading also in this case to an overestimation of the sum of spectroscopic factors with isotopic spin $T_>$ [10].

B. Shell model calculations

1. Negative parity

Negative parity levels have been calculated with the code ANTOINE [5], using the KB3G residual interaction in the full *pf* configuration space [28]. Five states for each spin value were calculated from $I = 1/2$ to $21/2$, making sure that all levels up to 4 MeV are included. All experimental energy levels up to 4 MeV are displayed in Fig. 6 for a comparison with SM predictions. It appears that all of them can be related to a

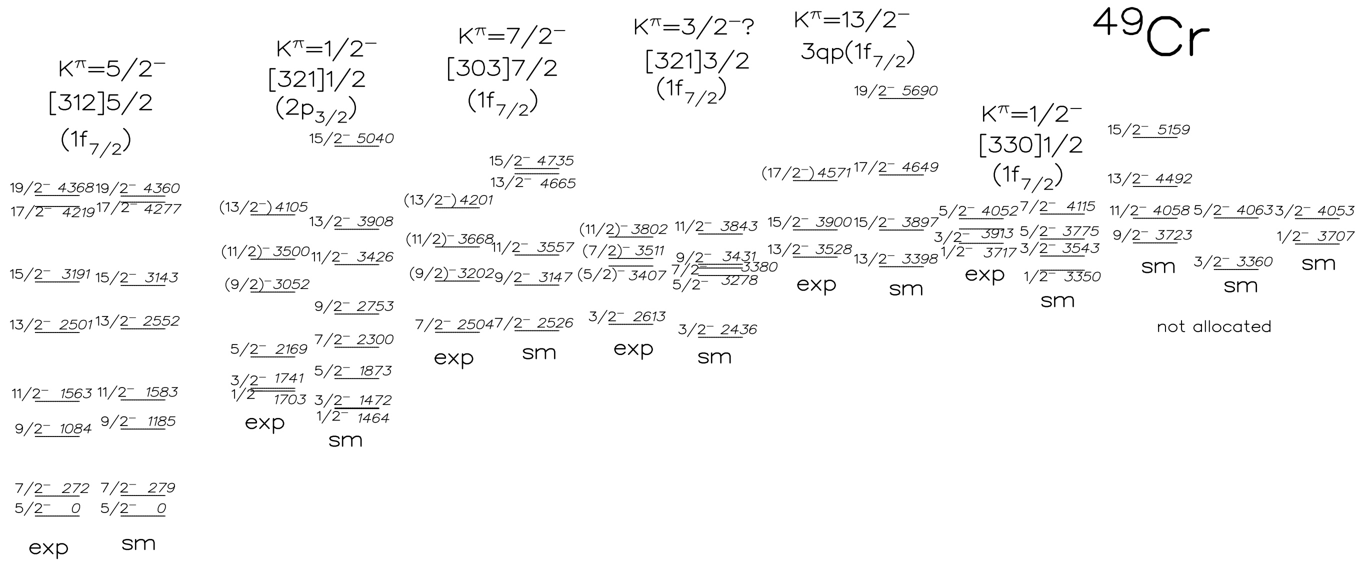

FIG. 6. Comparison of experimental negative parity levels with SM predictions.

theoretical level and that only a few predicted levels cannot be related to an experimental one. The tentative spin-parity assignments, reported in brackets in Fig. 6, rely in part on the predictive capability of SM calculations. One has to note, however, that the theoretical levels of the $K^\pi = 1/2^-$ band lie about 270 keV below the experimental ones.

SM $B(E2)$ and $B(M1)$ values are compared to the experimental ones in Table II. In the same table, the $B(E2)$ rotor values of Eq. (2) are also reported. The branching to the gs of the $(9/2)^-$ levels assigned to the bands with $K^\pi = 1/2^-$ and $7/2^-$ are assumed to be negligible on the basis of the SM estimates.

The decay towards the gs band of levels $1/2^-$, $3/2^-$, and $5/2^-$ of the $K^\pi = 1/2^-$ band is correctly predicted to be very small, in accordance with the K-selection rule.

The $7/2^-$ level at 2504 keV is not assigned to the $K^\pi = 1/2^-$ band, but to the $K^\pi = 7/2^-$ band based on the $[303]7/2^-$ orbital, because of its very fast decay. Its lifetime is, in fact, quoted to be shorter than 12 fs [2], while an upper limit of 30 fs is found in the present experiment. As reported in Table II, this agrees with the theoretical prediction of 3 fs for the lifetime of the $K^\pi = 7/2^-$ bandhead, while the alternative assumption ($K^\pi = 1/2^-$) would lead to the prediction of a lifetime of about 200 fs. The $B(M1)$ values for transitions of the $K^\pi = 7/2^-$ bandhead to the gs band are predicted to be of the order of one μ_N^2, confirming that no K-selection rule is active. On the contrary the K-selection rule explains the very small $B(M1)$ values of the low spin members of the $K^\pi = 1/2^-$ band. One can conclude that the wave function of the observed $7/2^-$ state has a prevailing $K = 7/2$ component.

A further spectroscopic tool is provided by the SM predictions for Q_s and g-factor values reported in Table III. They have in fact to be considered reliable estimates, on the basis of the agreement achieved for the level scheme and for the $B(E2)$ and $B(M1)$ values. In this context, the suggestion that the observed yrast $7/2^-$ level is a bandhead is confirmed by the large positive Q_s value of 31.7 $e\,\mathrm{fm}^2$ predicted by the SM [see Eq. (1)]. The SM g-factor value is small and positive, as in the PRM calculations. Since the rotor value is negative, some mixing is confirmed. No quenching of nucleon g factors is assumed in the SM calculations, which will be justified later.

While the lowest terms of the bands are firmly established and well reproduced by SM calculations, some uncertainty remains for higher terms, quoted in brackets in Fig. 6. While SM em moments agree with rotor properties and thus with the K-hindered decay from the $K = 1/2$ band, the observed decays of levels $9/2^-$ and $11/2^-$ of the $K = 1/2$ and 7/2 bands do not exhibit peculiar experimental differences, in disagreement with SM predictions. This is explained by the fact that if one increases by 270 keV the theoretical values for the $K^\pi = 1/2^-$ band in order to compensate the energy offset with respect to the experimental values, the theoretical energies of the levels $7/2^-$, $9/2^-$, $11/2^-$, and $13/2^-$ of the bands $K = 1/2$ and 7/2 get close, so they likely mix strongly. In this way, the $K = 1/2$ members may acquire from the $K = 7/2$ band a sizable $M1$ strength to the gs band. The adopted band assignments merely correspond to a slightly better correspondence between theoretical and experimental levels. The arising ambiguity is not explicit in Fig. 6. One of the two $(11/2)^-$ levels could be the $9/2^-$ level corresponding to that predicted at 3431 keV.

The $3/2^-$ level at 2613 keV is predicted by the SM at 2436 keV, but the Q_s value for the suggested head of the $K^\pi = 3/2^-$ band has the opposite sign of the rotor estimate. The SM g-factor value has a negative sign which reveals its neutron character, but the size is -0.40, i.e., about three times bigger than the rotor predictions for a $1f_{7/2}$ neutron. Moreover, it is predicted to be connected to a calculated $1/2^-$ level at 3707 keV with $B(E2) = 83\,e\,\mathrm{fm}^2$. This band does not have clear rotational features. This can be related to K mixing, which would be consistent with the observed strong signature splitting of the levels $(5/2)^-$ at 3407 keV and $(7/2)^-$ at 3511 keV (these levels were observed in transfer

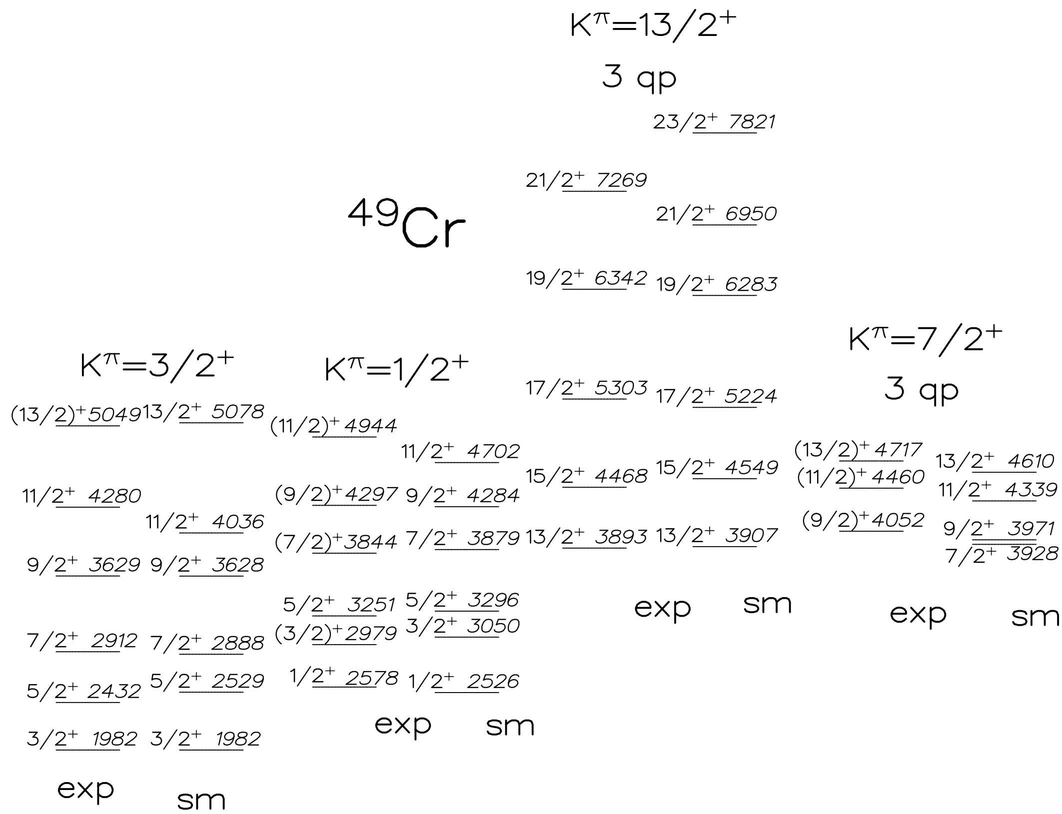

FIG. 7. Comparison of positive parity levels with SM predictions.

reaction with $l_n = 3$, so that the experimental assignment for both is $5/2^- - 7/2^-$). The $11/2^-$ level observed at 3802 keV probably corresponds to the calculated one at 3843 keV, which is predicted to be strongly connected to the $(7/2)^-$ level at 3511 keV.

The yrare $13/2^-$ level was already discussed in Ref. [3], where it was identified as the head of a $K^\pi = 13/2^-$ band. SM predicts in fact $Q_s = 55\,e$ fm^2. According to the rotor prediction of Eq. (1), its deformation would be about 20% lower than that of the gs band. Its calculated g factor is 0.77, which is about twice that of the corresponding yrast level, and indicates the two-proton alignment. A semiclassical estimate is obtained considering the sum of the projection of the unpaired nucleons' magnetic moment along the symmetry axis: $g_{13/2} = 2/13[1.4(5/2 + 3/2) - 0.40 \cdot 5/2] = 0.71$, which agrees with the SM values. A reduction of rotational collectivity is suggested by the lower contribution of the $2p_{3/2}$ orbital with respect to the gs band, calculated by the SM. In fact, it has been shown that the $2p_{3/2}$ orbital occupation is the essential ingredient that leads to deformation [5]. The breaking of a proton pair also reflects into a theoretical g-factor value larger than the rotor one. The levels $(15/2^-)$ and $(17/2^-)$ belonging to the $K = 13/2^-$ band are well characterized by their decay schemes.

A $K^\pi = 9/2^-$ band is predicted to be based on a $9/2^-$ level at 3723 keV. Its Q_s value is $55.7\,e$ fm^2, and it is connected to the $11/2^-$ levels at 4058 MeV with a $B(E2)$ value of 279 e^2 fm^4. The band continues with levels $13/2^-$ and $15/2^-$, but its nature is not yet understood.

2. *Positive parity*

Experimental and theoretical data for positive parity levels are reported in Tables I and II, together with those of negative parity levels. The experimental levels are compared with SM predictions in Fig. 7, where the excitation energy of the yrast $3/2^+$ is adjusted to the experimental value and where the $21/2^+$ and $23/2^+$ levels reported in Ref. [3] are also shown. The experimental bands with $K^\pi = 3/2^+$ and $K^\pi = 13/2^+$ have been already discussed in that reference, but now the $K = 3/2^+$ band has been substantially extended. They have been reproduced there with SM calculations, where one nucleon was lifted from the $1d_{3/2}$ orbital and three particles were allowed to be promoted from the $1f_{7/2}$ orbital to the rest of the pf configuration space. In this frame, the band $K^\pi = 13/2^+$ is described with a $\pi d_{3/2}^{-1} \otimes {}^{50}\mathrm{Mn}(K^\pi = 5^+, T = 0)$ configuration, where a parallel coupling occurs. This band should terminate at $33/2^+$, while levels are seen only up to $23/2^+$.

The same calculations predict, however, the yrast $1/2^+$ as 2 MeV too high. This is caused by the configuration space truncation, which does not account for the large contribution of the $2s_{1/2}$ orbital in the Nilsson orbital $[200]1/2^+$. This does not affect much the description of the $[202]3/2^+$ orbital, which is calculated by the particle-rotor model to have a nearly pure $1d_{3/2}$ configuration.

It is thus necessary to also allow a hole in the $2s_{1/2}$ orbital. The interaction is similar to that used for the $K^\pi = 3/2^+$ band in ^{47}V [29], with nearly standard values of binding energies. Satisfactory agreement is generally obtained for the level energies, while the $B(M1)$ values of some $K^\pi = 1/2^+$ band

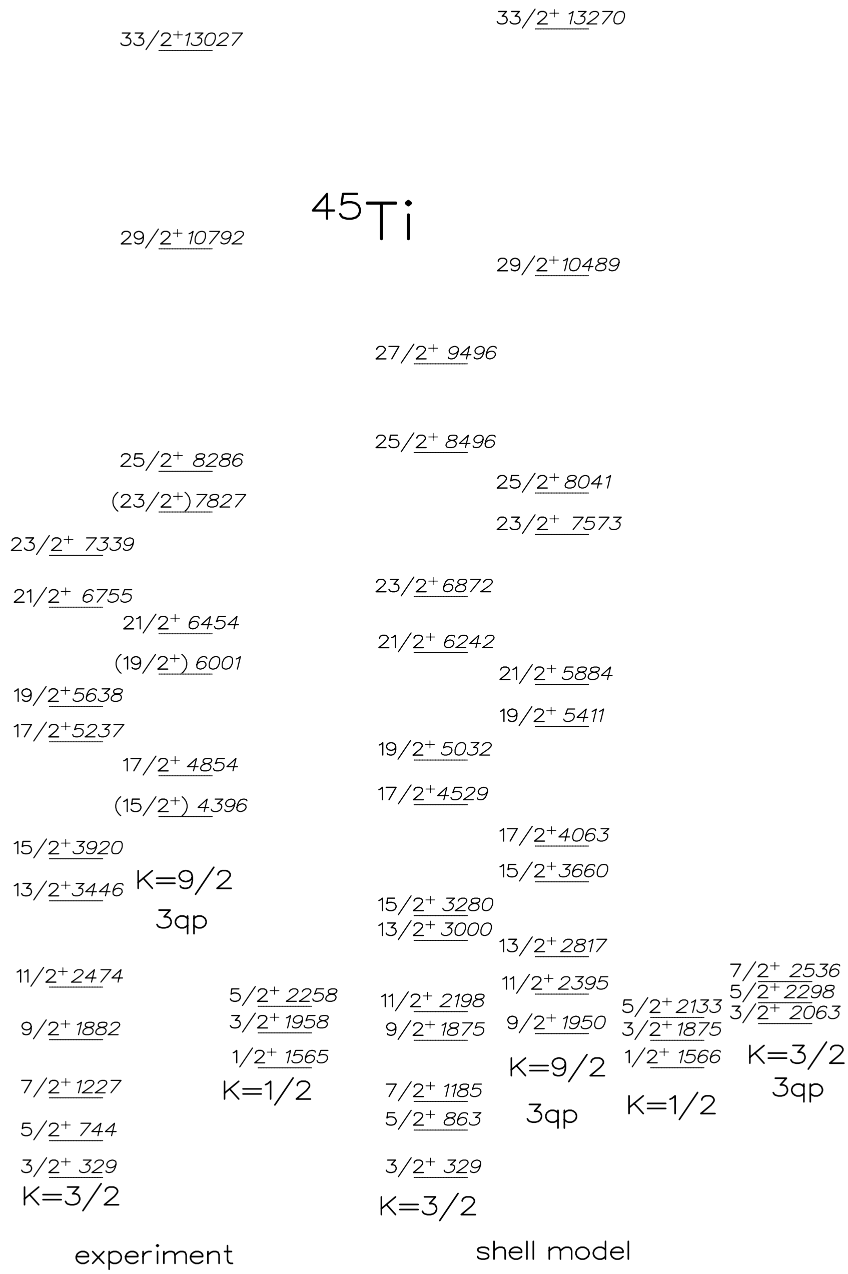

FIG. 8. Comparison of positive parity levels with SM predictions in ^{45}Ti.

members are predicted too large. The members of the latter band above 5/2$^+$ are not compared with theory in Table II because branchings to low members of the gs band could not be observed. A 3-*qp* band with $K^\pi = 7/2^+$ is predicted by SM in the case of an antiparallel coupling of spins. Its decay to the $K^\pi = 3/2^+$ one is predicted to occur mainly via $E1$ transitions to the gs band. There are a few candidates that belong to such a band, i.e., the levels at 4052, 4460, and 4717 keV that have rather long lifetimes in spite of the high energy of the depopulating γ rays. The level at 4052 keV is a candidate to be 9/2$^+$ by its peculiar decay. If this is the case, the bandhead 7/2$^+$ is very close in energy, but its decay to the first excited level was not observed.

A confirmation of the existence of core-excited 3-*qp* bands at low energies has been provided by the recent observation in ^{45}Ti of a sequence from 17/2$^+$ up to 33/2$^+$ [30], which can be described as the upper part of the $K^\pi = 9/2^+$ band because of the parallel alignment of three particles. Such a band can be described with the configuration $\pi d_{3/2}^{-1} \otimes {}^{46}\mathrm{V}(K = 3, T = 0)$, which terminates at 33/2$^+$ as the one in ^{49}Cr. The reason why termination was not seen in ^{49}Cr may be that a hole excitation requires nearly 2 MeV more. In ^{51}Mn, an intruder band $1g_{9/2}$ was observed rather than core-excited bands [31]. The comparison of SM predictions with observed positive parity levels in ^{45}Ti is shown in Fig. 8. Different to that observed in Ref. [30], a level (15/2$^+$) is located at 4396 keV by inverting the cascade following the decay of the 17/2$^+$ level. A 3-qp band with $K^\pi = 3/2^+$ is predicted but not yet observed.

TABLE IV. Comparison of experimental and theoretical g factors.

Nucleus	Level	$g_{\rm exp}$	$g_{\rm SM}^{\rm bare}$	$g_{\rm SM}^{\rm eff}$
^{49}V	7/2$^-$	1.277(5)	1.248	1.179
^{51}V	7/2$^-$	1.4710(5)	1.442	1.350
^{51}Mn	5/2$^-$	1.4273(5)	1.360	1.280
^{53}Mn	7/2$^-$	1.435(2)	1.386	1.332

C. About effective nucleon *g* factors

Bare values of the nucleon g factors are adopted in this paper; while in an earlier work [17] and in some recent papers, effective values of the nucleon g factor were used. In particular in Refs. [32] and [28], the following effective parameters were adopted in the shell *pf*: $g_s^{\rm eff} = 0.75 g_s^{\rm bare}$, $g_\ell(\pi)^{\rm eff} = 1.1$, and $g_\ell(\nu)^{\rm eff} = -0.1$, which were justified mainly based on electron-induced $M1$ excitation data [32]. One must, however, consider that g-factor values provide a better test for the assessment of effective values. In fact, in some cases, the experimental values are very precise and SM calculations predict very well the level scheme; while in the case of $M1$ excitation, one may suspect uncertainties in evaluating the experimental cross section and the sum rule of the $B(M1)$ values, which range over a large energy interval in which the quality of the SM calculations is not always good.

In Table IV, the comparison is limited to the odd-Z nuclei ^{49}V, ^{51}V, ^{51}Mn, and ^{53}Mn, for which the SM predictions are very good at low excitation energy. Assuming the bare nucleon g factors in the calculations, one gets an average precision of 5%; using the effective values results in considerably poorer agreement. It is inferred that in this major shell, where account is taken of both the dominant $\ell + 1/2$ and the conjugated $\ell - 1/2$ orbitals, there is no experimental evidence of the meson exchange current (MEC) effects on the nucleon g factors, which were discussed in Ref. [33]. In this context, the quenching of the nucleon g factor, which is usually applied to reduce the disagreement with experimental values of PRM calculations, appears to account roughly for the configuration mixing among the shell model orbitals.

A similar comparison for odd-N nuclei would not be conclusive since the predicted quenching is already small. The present conclusions confirm that of a recent paper [34], where the value $g_s^{\rm eff} = 0.9 g_s^{\rm bare}$ was derived from a comparison with SM of 113 experimental magnetic moments in the mass range $A = 47-72$. In the *sd* major shell, the evidence of the need for using effective values for the nucleon g factors to reproduce the experimental g factors is also not firm [35], and similar effective values as in Ref. [34] could be adopted. It is not yet understood, however, why the sum rule in $M1$ excitation processes requires, as mentioned, the use of strongly quenched g_s values.

One reason why quenching of nucleon g-factor operators due to MEC was often assumed is related to the quenching of the G_A coefficient in Gamow-Teller (GT) weak decay, which was recently deduced to be also about 0.75 [28]. The weak and em decays occur, in fact, via similar operators, since the GT operator is $\vec{\sigma}\tau$, while the magnetic moment operator is $\vec{\mu} = g_\ell^{\rm is}\vec{l} + 1/2 g_s^{\rm is}\vec{\sigma} + g_\ell^{\rm iv}\vec{l}\tau_z + 1/2 g_s^{\rm iv}\vec{\sigma}\tau_z$, where the superscripts is and iv refer to the isoscalar and isovector terms, respectively. In Ref. [34], the smallness of the global MEC effect on g-factor values was ascribed to the compensation of the quenching of the operator $\vec{\sigma}\tau_z$ with the MEC effects on the other operators. It was also observed that the operator $\vec{\sigma}\tau_z$ may experience different MEC effects in em and weak interactions [33,36].

V. CONCLUSIONS

The level scheme adopted for ^{49}Cr includes several new levels, which are displayed as thinner lines in Fig. 2. K^π values for nine sets of levels observed in this experiment are proposed. Six bands are described by the Nilsson configurations lowest in energy, where the K^π values suggested in the Nuclear Data Sheets [2] are confirmed for three of them. A clear correspondence is established between particle-rotor and shell model calculations. Moreover, three 3-*qp* bands are observed: the $K^\pi = (7/2^+)$ is new, the $K^\pi = 13/2^+$ is confirmed, and the $K^\pi = 13/2^-$ is substantially extended. SM calculations in the full *pf* configuration space account for all observed negative parity levels up to about 4 MeV. Calculations account reasonably well for all observed positive parity levels, extending the configuration space to include a nucleon-hole in either the $1d_{3/2}$ or $2s_{1/2}$ orbitals.

A comprehensive description of ^{49}Cr is presented. However, since some assignments are tentative, a measurement with a larger γ-detector array would be desirable in order to verify the proposed scenario. Moreover, measurement in coincidence with neutrons would allow one to also determine precisely the branches to the ground state, probably revealing the missing 7/2$^-$ level of the $K^\pi = 1/2^-$ band. Particularly challenging is to improve the knowledge of the 3-$qpK^\pi = (7/2^+)$ band.

This work showed that full spectroscopy is at hand and that it can be fruitful not to leave the still fertile stability valley for cultivating friable slopes. As a secondary-result, it is shown that in shell model calculations, the bare values of nucleon g factors are suitable for calculating magnetic effects.

ACKNOWLEDGMENT

R.V.R. thanks the Istituto Nazionale di Fisica Nucleare and Conselho Nacional de Desenvolvimento Cientifico e Tecnologico for financial support.

[1] G. Martinez-Pinedo, A. P. Zuker, A. Poves, and E. Caurier, Phys. Rev. C **55**, 187 (1997).
[2] T. Burrows, Nucl. Data Sheets **76**, 191 (1995).
[3] F. Brandolini *et al.*, Phys. Rev. C **60**, 041305(R) (1999).
[4] F. Brandolini *et al.*, Nucl. Phys. **A693**, 517 (2001).
[5] E. Caurier, J. L. Egido, G. Martinez-Pinedo, A. Poves, J. Retamosa, L. M. Robledo, and A. P. Zuker, Phys. Rev. Lett. **75**, 2466 (1995).
[6] F. Brandolini and C. A. Ur, Phys. Rev. C **71**, 054316 (2005).
[7] J. Kasagi *et al.*, Nucl. Phys. **A414**, 206 (1984).

[8] P. Bednarczyk *et al.*, Eur. Phys. J. A **2**, 157 (1998).
[9] F. Iachello, Phys. Rev. Lett. **85**, 3580 (2000).
[10] J. Kasagi *et al.*, J. Phys. Soc. Jpn. **43**, 741 (1977).
[11] R. Wirowski *et al.*, Nucl. Phys. **A586**, 427 (1995).
[12] J. A. Cameron, M. A. Bentley, A. M. Bruce, R. A. Cunningham, W. Gelletly, H. G. Price, J. Simpson, D. D. Warner, and A. N. James, Phys. Rev. C **44**, 1882 (1991).
[13] J. C. Wells and N. Johnson, Report No. ORNL-6689 (1991), p. 44.
[14] L. C. Northcliffe and R. F. Schilling, Nucl. Data, Sec. A **7**, 233 (1970).
[15] S. H. Sie *et al.*, Nucl. Phys. **A291**, 443 (1977).
[16] F. Brandolini and R. V. Ribas, Nucl. Instrum. Methods A **417**, 150 (1998).
[17] F. Brandolini *et al.*, Nucl. Phys. **A642**, 387 (1998).
[18] F. Brandolini *et al.*, Phys. Rev. C **64**, 044307 (2001).
[19] F. Brandolini *et al.*, Phys. Rev. C **66**, 024304 (2002).
[20] F. Brandolini *et al.*, Phys. Rev. C **66**, 021302(R) (2002).
[21] F. Brandolini *et al.*, Phys. Rev. C **70**, 034302 (2004).
[22] A. Bohr and B. R. Mottelson, *Nuclear Structure* (Benjamin, New York, 1975), Vol. 2, p. 45.
[23] K. E. G. Löbner, M. Vetter, and V. Hönig, Nucl. Data, Sec. A **7**, 495 (1970).
[24] S. E. Larson, G. Leander, and I. Ragnarsson, Nucl. Phys. **A307**, 189 (1978).
[25] F. Brandolini *et al.*, in *Experimental Nuclear Physics in Europe, Seville, Spain, 1999*, AIP Conf. Proc. no. 495 edited by B. Rubio, M. Lozano, and W. Gelletly (AIP, New York, 1999), p. 189.
[26] A. Juodagalvis and S. Aberg, Phys. Lett. **B428**, 227 (1998).
[27] Y. Fujita *et al.*, Nucl. Phys. **A435**, 7 (1985).
[28] A. Poves *et al.*, Nucl. Phys. **A694**, 157 (2001).
[29] A. Poves and J. S. Solano, Phys. Rev. C **58**, 179 (1998).
[30] P. Bednarczyk *et al.*, Eur. Phys. J. A **20**, 45 (2004).
[31] J. Ekman *et al.*, Phys. Rev. C **70**, 014306 (2004).
[32] P. von Neumann-Cosel *et al.*, Phys. Lett. **B443**, 1 (1998).
[33] B. Castel and I. S. Towner, *Modern Theories of Nuclear Moments* (Clarendon Press, Oxford, 1990).
[34] M. Honma, T. Otsuka, B. A. Brown, and T. Mizusaki, Phys. Rev. C **69**, 034335 (2004).
[35] B. A. Brown and B. H. Wildenthal, Annu. Rev. Nucl. Part. Sci. **38**, 29 (1988).
[36] Y. Fujita, B. A. Brown, H. Ejiri, K. Katori, S. Mizutori, and H. Ueno, Phys. Rev. C **62**, 044314 (2000).